Dynamics of femtosecond filamentation from saturation of self-focusing laser pulses

A. Couairon
Centre de Physique Théorique, CNRS UMR 7644, École Polytechnique, 91128 Palaiseau, France
(Received 26 February 2003; published 8 July 2003)

An interpretation is proposed for the dynamics of light filaments formed when a femtosecond laser pulse propagates in air. The pulse evolves as a set of coupled nonlinear oscillators forming a coherent structure over several Rayleigh lengths. The plasma generated by photoionization is numerically shown to be the single saturation mechanism of the beam self-focusing. Other physical processes such as group velocity dispersion and the quintic susceptibility $\chi^{(5)}$ for the polarization promote different propagation regimes. From theoretical expressions of the oscillation period for the spatial profile of the pulse, we show that the electron density in a femtosecond filament may be estimated.

DOI: 10.1103/PhysRevA.68.015801 PACS number(s): 42.65.Sf, 42.25.Bs, 42.65.Jx, 52.38.Hb

When an ultrashort laser pulse propagates in a transparent Kerr medium, the beam with an input power larger than the self-focusing threshold P_{cr} first self organizes to form, beyond a nonlinear focus, a narrow coherent structure. This structure, called a light filament, excites in its wake an electron plasma by light induced ionization. Femtosecond filaments have been observed in gases as air [1], in solids as silica glasses [2] and in liquids [3]. Light filaments are not only interesting in themselves: their unusually long propagation distance compared to the Rayleigh length has attracted considerable attention since it suggests that a significant part of the pulse energy can be transported as ''light bullets.'' Several applications such as remote sensing in the atmosphere [4] or lightning protection [5,6] rely on this interesting property, while others, such as the generation of ultrashort secondary sources, merely rely on the production of a tenuous plasma channel [7,8].

Since the first observation of infrared filaments in air by Braun *et al.* [1], several mechanisms have been reported to explain why they sustain over long distances. A balance between the optical Kerr effect, the beam diffraction, and the defocusing effect owing to multiphoton ionization of air was first proposed in Ref. [1] so that a leaky waveguide [9] is formed. Light filaments have then been shown numerically to propagate according to a dynamical equilibrium between these three physical effects [10–12]. The intensity around 10^{14} W/cm^2 and the electron density of 10^{16} cm^{-3}, estimated from a simple dimensional analysis, although in agreement with measurements of these quantities [13,14], are maximum values reached periodically along the propagation axis. Ultraviolet light filaments have also been observed in air [15,16], and the mechanism regularizing the propagation is likely to be identical for ultraviolet and infrared pulses [17].

Beam self-focusing (SF) due to the optical Kerr effect plays a key role in femtosecond filamentation in transparent media, since it overcomes diffraction for pulses with power above critical. In a purely Kerr medium, a collapse singularity occurs at a finite propagation distance, which may be estimated from Marburger's formula [18]. In a real medium, a specific physical effect counterbalances or simply act against SF. The collapse process is then arrested and a subsequent propagation regime takes place in the form of a dynamical equilibrium between this physical effect and SF. The nature of this effect and the possible subsequent propagation in the form of a spatiotemporal soliton is still controversial in the literature [19,20]. Plasma defocusing acts not only as a higher-order nonlinearity which saturates SF locally when an electron plasma is generated by photoionization, but also as a global effect coupling the various parts of the pulse. In addition to this effect, various processes have been proposed as potential candidates for regularizing the collapse of ultrashort laser pulses. Among them, normal group-velocity dispersion (GVD) is known as promoting pulse splitting, that leads to the sharing of the temporal profile of the pulse into two symmetric subpulses [21–24]. Although it does not saturate SF, GVD shifts the power threshold for the collapse [25]. Saturation by a quintic susceptibility term in the nonlinear polarization ($\chi^{(5)}$) was also proposed in [26]. For one-dimensional propagation, $\chi^{(5)}$ effects promote the formation of solitary waves.

In the present paper, we show that a femtosecond light filament is a long range propagating coherent structure resulting from the saturation of self-focusing by a single mechanism: photoionization. This process leads to asymmetric pulse temporal profiles and spectra, while other propagation regimes lead to symmetric modulated pulses and are therefore not compatible with femtosecond filamentation. An estimation of the electron density is obtained from the oscillation period for the pulse intensity. These results lead, to our knowledge, to a new interpretation of femtosecond filamentation in air.

Although we present a general model describing the propagation of an ultrashort laser pulse in a dispersive transparent medium, only the principle physical effects possibly leading to the arrest of collapse and femtosecond filamentation are considered. The linearly polarized electric field of the incident beam propagates along the z axis. It is decomposed into a carrier wave with frequency ω_0 and wave number $k \equiv n_0 \omega_0 / c$, where n_0 denotes the linear index of refraction of the medium and a slowly varying amplitude as $\mathbf{E} = \mathrm{Re}[\boldsymbol{\mathcal{E}} \exp(ikz - i\omega_0 t)]$. The scalar envelope $\mathcal{E}(x,y,\tau,z)$ evolves according to the propagation equation expressed

in the reference frame moving at the group velocity $v_g \equiv \partial\omega/\partial k|_{\omega_0}$:

$$\frac{\partial \mathcal{E}}{\partial z} = \frac{i}{2k}\left(\frac{\partial^2}{\partial x^2} + \frac{\partial^2}{\partial y^2}\right)\mathcal{E} - i\frac{k''}{2}\frac{\partial^2 \mathcal{E}}{\partial \tau^2} + ik_0\frac{\Delta n}{n_0}\mathcal{E}, \qquad (1)$$

where τ refers to the retarded time variable $t - z/v_g$. The first and second terms on the right-hand side of Eq. (1) account for diffraction within the transverse plane and GVD with coefficient $k'' \equiv \partial^2 k/\partial\omega^2|_{\omega_0}$. Below, we consider propagation in air for which $k'' = 0.2$ fs^2/cm at 800 nm. The quantity $\Delta n/n_0$ describes the local saturable index change and may include various components as:

(i) $\Delta n/n_0 = n_2|\mathcal{E}|^2$ describing the self-focusing related to the Kerr effect with nonlinear refraction index of air $n_2 = 4 \times 10^{-19}$ cm^2/W. The critical power for self-focusing is $P_{\rm cr} = \lambda_0^2/2\pi n_2 \simeq 2.5$ GW. For the sake of simplicity, the effect of the delayed component in the Kerr response of nitrogen, due to impulsive Raman excitation of rotational coherences [27] is not taken into account. Below, we indicate the modifications this effect would induce.

(ii) $\Delta n/n_0 = -n_4|\mathcal{E}|^4$ describing a stabilizing high-order nonlinearity depending on the quintic susceptibility of the nonlinear medium through $n_4 \equiv \chi^{(5)}/2n_0$. In air $n_4 \sim 10^{-32}$ cm^4/W^2 as suggested in [26].

(iii) $\Delta n/n_0 = -i\rho/2\rho_c$ describing the defocusing due to the plasma with electron density ρ created by photoionization. Here, $\rho_c = 1.8 \times 10^{21}$ cm^{-3} denotes the critical plasma density. A general formulation has been given by Keldysh [28] to describe photoionization. Without loss of generality, we will consider the multiphoton limit corresponding to intensities smaller than 10^{14} W/cm^2.

Multiphoton ionization (MPI) of the medium with neutral atom density $\rho_{\rm air} = 2.7 \times 10^{19}$ cm^{-3} is described by an evolution equation for the electron density ρ

$$\frac{\partial \rho}{\partial \tau} = \sigma_K I^K(\rho_{\rm at} - \rho), \qquad (2)$$

where $K \equiv \mathrm{mod}(U_i/\hbar\omega_0 + 1)$ is the number of photons that must be absorbed by an atom with ionization potential U_i to liberate an electron. For intensities smaller than 10^{14} W/cm^2, it is sufficient to consider oxygen ionization with potential $U_{\rm O} = 12.1$ eV and initial density $\rho_{\rm at} = 0.2\rho_{\rm air}$, since it prevails over nitrogen ionization with $U_{\rm N} = 15.6$ eV. The ionization rate $\sigma_K I^K$ is computed from Keldysh's theory in the multiphoton limit with $K = 8$ for oxygen and $\sigma_K = 3.7 \times 10^{-96}$ s^{-1} cm^{16}/W^8 at the laser wavelength $\lambda_0 = 800$ nm.

The input beams are modeled by collimated Gaussians with peak intensity I_0, a waist $w_0 = 0.5$ mm, a temporal half width $t_p = 50$ fs, an energy $E_{\rm in} = P_{\rm in} t_p \sqrt{\pi/2} = 1$ mJ and a peak power $P_{\rm in} = \pi w_0^2 I_0/2 = 7.4 P_{\rm cr}$:

$$\mathcal{E}(x, y, \tau, 0) = \sqrt{I_0}\exp[-(x^2 + y^2)/w_0^2 - \tau^2/t_p^2]. \qquad (3)$$

First we estimate which physical effect among GVD, MPI, and the saturating quintic nonlinearity ($\chi^{(5)}$) most likely regularizes the collapse. By MPI we also mean the associated plasma-defocusing term. For the nonlinear Schrödinger equation (1), the collapse proceeds from the self phase modulation induced by the Kerr effect. Physical effects that do not directly act on the phase such as, e.g., energy absorption, cannot regularize the collapse and therefore have not been taken into account. The question of whether an equilibrium occurs between SF and another physical effect will be answered to by using physical scales as w_0, t_p, $P_{\rm in}$, I_0 and by estimating crudely the electron density as $\rho = \sigma_K I_0^K \rho_{\rm at} t_p$. (i) SF and diffraction: $P_{\rm in} = P_{\rm cr}/8$. (ii) SF and MPI: $I_0 = I_{\rm MPI}^{\rm Sat} \equiv (2\rho_c n_2/\rho_{\rm at}\sigma_K t_p)^{1/(K-1)}$. (iii) SF and GVD: $I_0 = k''/2k_0 n_2 t_p^2$. (iv) SF and $\chi^{(5)}$: $I_0 = I_{\chi^{(5)}}^{\rm sat} \equiv n_2/n_4$. Other equilibria are given by the balance between diffraction and GVD, $I_0 = 2P_{\rm in}k_0 k''/\pi t_p^2$, and that between diffraction and MPI: $I_0 = (\pi\rho_c/2P_{\rm in}k_0^2\rho_{\rm at}\sigma_K t_p)^{1/(K-1)}$.

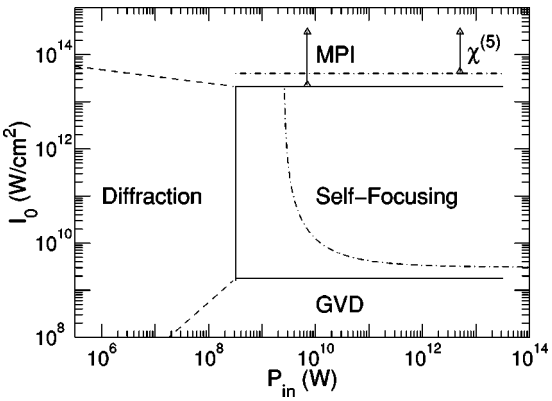

FIG. 1. Prevailing physical effect as functions of the pulse intensity and input power. The continuous lines mark the self-focusing region bounded by the equilibrium with MPI (from above), GVD (from below) and diffraction at $P_{\rm cr}/8$.

Figure 1 shows the different domains where one of the above mentioned physical effects prevails. Self-focusing dominates over diffraction for $P_{\rm in} > P_{\rm cr}/8$. In the absence of any nonlinear saturating effect, SF leads to the collapse of the beam for $P_{\rm in} > P_{\rm cr}$ [18].

As shown in Ref. [25], for $P_{\rm in}$ slightly above $P_{\rm cr}$, a pulse splitting due to the conjugated action of self-phase modulation and GVD can arrest the collapse: GVD leads to the spreading to neighboring slices of the power contained in the collapsing central time slices of the pulse. The splitting process starts when the power in the central slice is reduced to subcritical since diffraction dominates in this slice while SF still dominates in the neighboring slices. This can occur, however, only below the dash-dotted curve in Fig. 1 (limit given in [25]). Self-focusing prevails over GVD at a large power and intensity. For input powers $P_{\rm in}$ and initial intensities I_0 above the dash-dotted curve, GVD stretches the pulse too slowly (in air k'' is small) during the SF process to stop the collapse, which occurs unless it becomes saturated by a higher order nonlinear effect. MPI for example, prevails over self-focusing above the continuous horizontal line in Fig. 1; $\chi^{(5)}$ leads to a similar saturation at a larger intensity (horizontal dash-dotted line) with the parameters of air. In this region, however MPI shadows $\chi^{(5)}$. For completeness, the balances between MPI, diffraction, and dispersion are

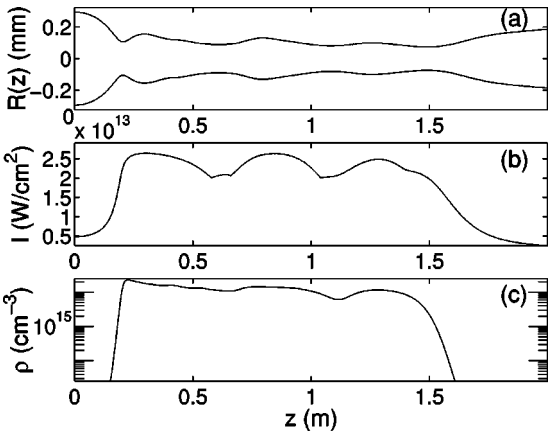

FIG. 2. (a) Averaged radius of the filament, (b) peak intensity and (c) electron density on axis $x=y=0$ for the saturation regime induced by MPI.

shown in dashed lines at low powers. The physical effect with the lowest saturation intensity prevails in regularizing the collapse and arresting the self-focusing process.

We have numerically computed the pulse propagation when all the components of the saturable index are included in Eq. (1), with input condition (3) for $P_{\text{in}}=7.4\,P_{\text{cr}}$. The averaged beam radius, the maximum intensity and the electron density are shown in Fig. 2 as a function of the propagation distance. During a short self-focusing stage, the Kerr effect prevails and the beam shrinks in the transverse diffraction plane. Then, an electron plasma is triggered by optical field ionization in the trailing part of the pulse and thereby saturates locally the Kerr effect. This saturation forms a light filament of diameter around 200 μm and preserves this robust long living coherent structure which can be viewed as a self-guided packet of light propagating over more than 30 Rayleigh lengths ($z_R\equiv\pi w_f^2/\lambda_0=3.9$ cm with $w_f=100$ μm). The maximum intensity about 2×10^{13} W/cm^2 and maximum density of 2×10^{16} cm^{-3} are in quite good agreement with the values roughly estimated by $\rho_{\max}/2\rho_c=n_2 I_{\max}$ and $\rho_{\max}=\sigma_K I_{\max}^K \rho_{\text{at}} t_p$.

The situation is different when only self focusing and the quintic nonlinearity $\chi^{(5)}$ are taken into account. The beam radius and the maximum intensity obtained numerically for the same input pulse as that in Fig. 2 are plotted in Fig. 3. In this simulation, the plasma generation was turned off. Saturation around 4×10^{13} W/cm^2, also in quite good agreement

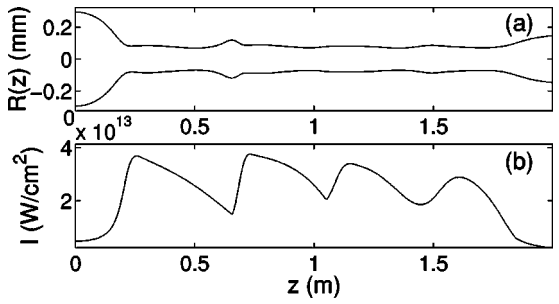

FIG. 3. (a) Averaged radius of the filament, (b) peak intensity on axis $x=y=0$ for the saturation regime induced by $\chi^{(5)}$.

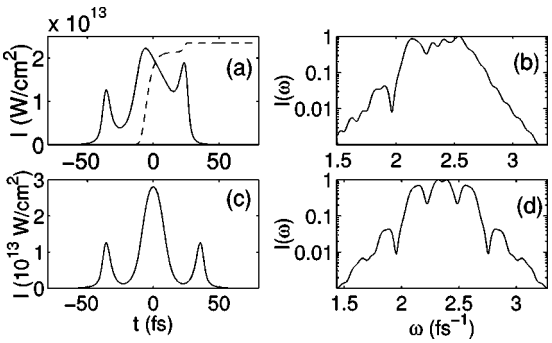

FIG. 4. Pulse intensity on axis $x=y=0$ as a function of time at $z=0.7$ m when (a) plasma defocusing and (c) quintic saturation balances the Kerr effect. The corresponding power spectra are show in (b) and (d).

with the value predicted in Fig. 1, $I_{\chi^{(5)}}^{\text{sat}}=n_2/n_4$, reflects the interplay between cubic and quintic nonlinearities. This demonstrates that once a physical effect saturates the self-focusing process, it prevents other saturation mechanisms with higher thresholds to play their role. Although the value for n_4 in [26] is only estimated, the result is the same when n_4 is such that $I_{\chi^{(5)}}^{\text{sat}}<I_{\text{MPI}}^{\text{sat}}$. A simulation in this case shows than $\chi^{(5)}$ is the single saturation mechanism. In some media, third order cascades dominate $\chi^{(5)}$ [29], and may then act as the dominant saturating process. Note that when the delayed Kerr effect is taken into account, it does not play the role of a saturating mechanism, does not prevent the collapse but only shifts its position toward positive z and induces self-phase modulation with spectral redshifting [27].

The effective saturation mechanism in femtosecond filamentation may be determined by direct inspection of the symmetry in the temporal profile and the power spectrum of the pulse. Figure 4 shows profiles and spectra computed at the same propagation distance $z=70$ cm in both cases. Figures 4(a) and 4(b) correspond to the simulation with both MPI and $\chi^{(5)}$ whereas only $\chi^{(5)}$ is present for Figs. 4(c) and 4(d). In Fig. 4(a), the electron density shown in dashed line has defocused the trailing part of the pulse, and SF has reformed a multipeaked structure. The three spikes indicate that different time slices with powers above critical have reached the end of a focusing stage at nearly the same distance. Here we propose an interpretation of femtosecond filamentation in air: The various time slices with power $P(t)$ above critical constitute a set of coupled spatial solitons. They oscillate slowly with different periods $Z(t)$ depending on the coupling and all the longer since $P(t)$ is close to P_{cr}. A time modulated, multipeaked pulse generically results from the coincidence on the propagation axis of the focal points belonging to several time slices. Since the saturating nonlinearity (the electron density front) is asymmetric in time, an asymmetric modulation results from the propagation. In Fig. 4(c), the same saturation phenomena occur: the pulse becomes modulated along propagation but the $\chi^{(5)}$ nonlinearity does not break the time symmetry. The oscillation period for the spatial profile of each time slice may be estimated by neglecting GVD as $Z(t)=4z_R\int_{u_m}^1 du/\sqrt{V(1)-V(u)}$, where $u_m=R_m/R_M$ denotes the ratio between minimal and maxi-

mal radii,

$$z_R = \pi R_M^2 n_0/\lambda_0, \quad V(u) = c(t)/u^{2K} - [P(t)/P_{\rm cr} - 1]/u^2,$$

$$c(t) = z_R k_0 (\rho_{\rm sat}/\rho_c)[P(t)R_m^2/2P_{\rm cr}R_M^2]^K[\sqrt{\pi K/2}/(K+1)^2],$$

and $K=8$ for the saturation by MPI, whereas $c(t) = n_4 I_{\rm sat} P(t) R_m^2/6n_2 P_{\rm cr} R_M^2$ and $K=2$ for the saturation by $\chi^{(5)}$. A time resolved measurement of the intensity profiles would confirm the multipeaked asymmetric structure of the pulse while the oscillation period of the spatial profile would yield an all optical measurement of the plasma density. The above formula for the central slice ($t=0$) with power $P_{\rm in}$, $R_m = 80\ \mu$m, $R_M = 160\ \mu$m, and a period $Z=40$ cm yields the density $\rho_{\rm sat} = 1.5\times 10^{16}\ {\rm cm}^{-3}$, in excellent agreement with the simulation displayed in Fig. 2(c). By using short pulses with different duration or wavelength, it may be possible to ensure $I^{\rm sat}_{\chi^{(5)}} < I^{\rm sat}_{\rm MPI}$, so that measurements of the oscillation period $Z(t)$ allow an estimation of the value of $\chi^{(5)}$ (or n_4). Pulse splitting such as that displayed in Figs. 4(a) and 4(c) leads to interference fringes in the pulse spectra [see Figs. 4(b) and 4(d) and, e.g., Ref. [2] for experimental evidence of such splitting in silica glasses]. The period between fringes is typical of the delay between the components in the temporal profile of the pulse, but not of the physical mechanism responsible for the splitting. This mechanism is ionization when the spectra are blueshifted [Fig. 4(b)] and $\chi^{(5)}$ when they are symmetrically broadened. In gases subject to self-phase modulation associated with the delayed Kerr effect, this effect induces redshifting which may, however, shadow the spectral blueshifting due to ionization.

In conclusion, we have proposed a new model of femtosecond filamentation in air. We have thoroughly characterized the saturation mechanism that enables light filaments to sustain over long distances. Only photoionization stops the collapse and the generated plasma bounds the growth of the intensity locally. A time-asymmetric modulated structure with a blueshifted spectrum is formed along propagation, since each time slice undergoes focusing-defocusing cycles with a period depending on the power it contains and the plasma density obtained at saturation. Although intrinsically difficult to perform in view of the high intensity present in the filament, measurements of the beam diameter oscillations might provide an indirect estimation of the plasma density in the wake of the pulse. This method generally applies to a determination of the susceptibility of the dominant saturating process such as, e.g., $\chi^{(5)}$ when it prevails over ionization. The model can be generalized to describe multifilamentation patterns resulting from the propagation in air of powerful ultrashort laser pulses, as their spatial dynamics is equivalent to the temporal dynamics shown in Fig. 4.

[1] A. Braun *et al.*, Opt. Lett. **20**, 73 (1995).
[2] S. Tzortzakis *et al.*, Phys. Rev. Lett. **87**, 213902 (2001).
[3] A. Dubietis, G. Tamosauskas, I. Diomin, and A. Varanavicius, Opt. Lett. **28**, 269 (2003).
[4] L. Wöste *et al.*, Laser Optoelektron. **29**, 51 (1997).
[5] F. Vidal *et al.*, IEEE Trans. Plasma Sci. **28**, 418 (2000).
[6] X.M. Zhao, J.-C. Diels, C.Y. Wang, J.M. Elizondo, IEEE J. Quantum Electron. **31**, 599 (1995).
[7] C.-C. Cheng, E.M. Wright, and J.V. Moloney, Phys. Rev. Lett. **87**, 213001 (2001).
[8] T. Brabec and F. Krausz, Rev. Mod. Phys. **72**, 545 (2000).
[9] E.T.J. Nibbering *et al.*, Opt. Lett. **21**, 62 (1996).
[10] H.R. Lange *et al.*, Opt. Lett. **23**, 120 (1998).
[11] M. Mlejnek, M. Kolesik, J.V. Moloney, and E.M. Wright, Phys. Rev. Lett. **83**, 2938 (1999).
[12] A. Couairon *et al.*, J. Opt. Soc. Am. B **19**, 1117 (2002).
[13] B. La Fontaine *et al.*, Phys. Plasmas **6**, 1615 (1999).
[14] S. Tzortzakis *et al.*, Phys. Rev. Lett. **86**, 5470 (2001).
[15] S. Tzortzakis *et al.*, Opt. Lett. **25**, 1270 (2000).
[16] J. Schwarz *et al.*, Opt. Commun. **180**, 383 (2000).
[17] A. Couairon and L. Bergé, Phys. Rev. Lett. **88**, 135003 (2002).
[18] J.H. Marburger, Prog. Quantum Electron. **4**, 35 (1975).
[19] I.G. Koprinkov, A. Suda, P. Wang, and K. Midorikawa, Phys. Rev. Lett. **84**, 3847 (2000).
[20] A.L. Gaeta, Phys. Rev. Lett. **84**, 3582 (2000); A.L. Gaeta and F. Wise, *ibid.* **87**, 229401 (2001).
[21] A.A. Zozulya, S.A. Diddams, A.G. van Engen, and T.S. Clement, Phys. Rev. Lett. **82**, 1430 (1999).
[22] P. Chernev and V. Petrov, Opt. Lett. **17**, 172 (1992); J.E. Rothenberg, *ibid.* **17**, 583 (1992).
[23] V. Tikhonenko, J. Christou, and B. Luther-Davies, Phys. Rev. Lett. **76**, 2698 (1996).
[24] J.K. Ranka, R.W. Schirmer, and A.L. Gaeta, Phys. Rev. Lett. **77**, 3783 (1996).
[25] G.G. Luther, J.V. Moloney, A.C. Newell, and E.M. Wright, Opt. Lett. **19**, 862 (1994).
[26] N. Aközbek, C.M. Bowden, A. Talebpour, and S.L. Chin, Phys. Rev. E **61**, 4540 (2000).
[27] G. Korn *et al.*, Phys. Rev. Lett. **81**, 1215 (1998).
[28] L.V. Keldysh, Zh. Éksp. Teor. Fiz. **47**, 1945 (1964) [Sov. Phys. JETP **20**, 1307 (1965)].
[29] D.A. Blank *et al.*, J. Chem. Phys. **111**, 3105 (1999).